# Assessment of three WENO type schemes for nonlinear conservative flux functions

Alina BOGOI[1], Sterian DANAILA*,[1], Dragos ISVORANU[1]

*Corresponding author
[1]Department of Aerospace Engineering, University Politehnica of Bucharest
Splaiul Independenţei 313, 060042, Bucharest, Romania
bogoi_alina@yahoo.com, sterian.danaila@upb.ro*, ddisvoranu@gmail.com

DOI: 10.13111/2066-8201.2018.10.1.18

*Received: 24 December 2017/ Accepted: 08 February 2018/ Published: March 2018*


***Abstract:*** *This paper focuses on a new comparison of the behavior of three Weighted Essentially Non-Oscillatory (WENO) type numerical schemes for three different nonlinear fluxes, in the case of scalar conservation law. The analytical solution is provided for various boundary conditions. For the time integration we adopt the 4-6 stage Low-Dispersion Low-Dissipation Runge-Kutta method (LDDRK 4-6). The schemes were tested on piecewise constant function for non-periodical conditions. The assessment was performed because the specialized literature mainly presents cases favorable illustrating only to a particular method while our purpose is to objectively present the performance and capacity of each method to simulate simple cases like scalar conservation law problems. All the schemes accurately identify the position of the shock and converge to the proper weak solution for the non-linear fluxes and different initial conditions. The paper is a continuation of the efficiency and accuracy analysis of high order numerical schemes previously published by the authors [1,2].*

***Key Words:*** *Conservative law, Riemann problem, WENO-type schemes, Runge-Kutta schemes*

## 1. INTRODUCTION

Many fluid dynamics applications from turbulence or acoustics include propagation of nonlinear waves with a continuous or discontinuous distribution of the physical variables. Rarefaction fans, shocks or contact discontinuities are elementary waves that build the solution of Riemann problem for hyperbolic equations, like Euler equations. The solution of the Riemann problem with two initial states, for a scalar conservation law and a convex flux is either a jump or a fan [1-4]. The wave type is determined by the entropy condition. In the case of a conservation law with a non-convex flux function, the Oleinik entropy condition is used to select the only physically admissible solution [5]. Contrary from a convex flux function problem, in the non-convex case it is possible that, depending on the number of inflection points, the solution of the Riemann problem contains not only an individual wave but a combination of two or three of these simple waves. The aim of the present work is to perform, for the first time, a new comparison of the behavior of three WENO-type numerical methods (the classical WENO [6, 7], the mapped WENO [8] and the compact reconstruction WENO [9]) with respect to the exact explicit solutions of the problem of Buckley-Leverett [10, 11] and the problem proposed by Harten [6] for different boundary conditions. We have chosen WENO schemes of fifth order of accuracy because we use non-periodical initial

conditions and in this context we need just two appropriate boundary closures at each end of a domain. Let us consider the initial value problem of the one-dimensional scalar conservative equation $\forall t \geq 0,\ x \in \mathbf{R}$:

$$\frac{\partial u}{\partial t}(x,t) + \frac{\partial f}{\partial t}\big[u(x,t)\big] = 0, \quad u(x,0) = u_0(x)\,, \tag{1}$$

where $u(x,t)$ is a conserved quantity, $f[u(x,t)]$ represents its flux and $u_0(x)$ is the initial condition. The numerical solution is obtained by discretizing the equation in space and time.

Discretizing the spatial derivative for each corresponding point $x_j = j\Delta x,\ j = \overline{0,N}$, the following conservative finite difference scheme yields:

$$\frac{\mathrm{d}u_j}{\mathrm{d}t} + \frac{\hat{f}_{j+1/2} - \hat{f}_{j-1/2}}{\Delta x} = 0. \tag{2}$$

Thus, we get a system of ordinary differential equations for $u_j(t) = u(x_j,t)$. The term $\hat{f}_{j+1/2}$ is the numerical flux satisfying the consistency requirements $\hat{f}_{j+1/2} = \hat{f}(u_{j-r},...,u_{j+s})$ and $\hat{f}(u,...,u) = f(u)$.

Following Shu and Osher [7], such a function is defined implicitly as

$$f(x) = \frac{1}{\Delta x}\int_{x-\Delta x/2}^{x+\Delta x/2} \hat{f}(\xi)\mathrm{d}\xi\,, \quad \left.\frac{\partial f}{\partial x}\right|_{x=x_j} = \frac{\hat{f}(x_{j+1/2},t) - \hat{f}(x_{j-1/2},t)]}{\Delta x}\,. \tag{3}$$

The solution of the conservative finite difference formulation of eq. (1) written in the semi-discrete form, eq. (2), consists of two steps: spatial discretization and time marching, respectively.

## 2. SPATIAL DISCRETIZATION

In the frame of spatial discretization, we are interested in the approximate reconstruction with a desired order of accuracy, $f(x) = \hat{f}(x) + \mathrm{O}\big[(\Delta x)^k\big]$, by using a polynomial with undetermined coefficients. Substitution of this polynomial into eq. (3) leads to a system of equations where the time integration can be performed.

The linear approximation for a numerical flux may be insufficient, especially when the solution has non-smooth behavior (such expansions, shocks or contact discontinuities). Therefore, numerical schemes based on linear approximation often produce spurious oscillations and overshoots near discontinuities. These nonphysical representations are known as weak or nonlinear instabilities.

A class of methods which satisfy nonlinear stability conditions in the sense that the magnitudes of any oscillations decay at $(\Delta x)^k$, where $k$ is the order of accuracy are WENO schemes [6-10].

We present briefly the basics of these schemes. A combination of stencils/polynomials of equal order and hence equal number of stencil points are used for any $r = \overline{0,k-1}$: $S_r(i) = \{f_{i-r}, f_{i-r+1},...,f_{i-r+k-1}\}$. However, the stencil points used have different levels of upwind and downwind bias. In smooth regions, a weighted combination of all stencils is used. For

ENO methods, where oscillations are detected, one member of the family of stencils is used. The least oscillatory is selected. For WENO, at oscillations the full family is used through the convex combination of interpolated values $f_{i+1/2}^{r}$:

$$f_{i+1/2} = \sum_{r=0}^{k-1} \omega_r f_{i+1/2}^{r} + O\left[(\Delta x)^k\right], r = \overline{0, k-1}, \tag{4}$$

where, for each stencil

$$f_{i+1/2}^{r} = \sum_{j=0}^{k-1} c_{rj} f_{i-r+j}\ ,\ r, j = \overline{0, k-1} \tag{5}$$

and $c_{rj}$ can be found in [7, 10]. The weights $\omega_r$ are defined as $r = \overline{0, k-1}$

$$\omega_r = a_r \ / \sum_{k=0}^{k-1} a_l\ \ , a_r = d_r\ / (\varepsilon + \beta_r)^p, \tag{6}$$

where the tiny parameter $\varepsilon$ ($\varepsilon \approx 10^{-6}$) is introduced to avoid the denominator to become zero. The ideal weights, $d_r$, assure that in smooth regions the value $u_{i+1/2}$ is approximated to order $O\left[(\Delta x)^{2k-1}\right]$ and present a non-oscillatory behavior near discontinuities, [10]. However, in the vicinity of the critical points (where the first or higher derivatives vanish) the solution strongly depends on the assumed value of $\varepsilon$, even for smooth data.

The smoothness indicator $\beta_r$, $r = \overline{0, k-1}$, is given by:

$$\beta_r = \sum_{m=1}^{k-1} \int_{x_{i-1/2}}^{x_{i+1/2}} \Delta x^{2m-1} \left( \frac{\mathrm{d}^m p_r}{\mathrm{d}x^m} \right)^2 \mathrm{d}x, \tag{7}$$

$p_r$ being the interpolation polynomial over the interval $I_i = [x_{i-1/2}, x_{i+1/2}]$.

For example, for WENO5, $k = 3$ yield:

$$\begin{cases} \beta_0 = 13\left(f_i - 2f_{i+1} + f_{i+2}\right)^2 / 12 + \left(3f_i - 4f_{i+1} + 3f_{i+2}\right)^2 / 4, \\ \beta_1 = 13\left(f_{i-1} - 2f_i + f_{i+1}\right)^2 / 12 + \left(f_{i-1} - f_{i+1}\right)^2 / 4, \\ \beta_2 = 13\left(f_{i-2} - 2f_{i-1} + u_i\right)^2 / 12 + \left(f_{i-2} - 4f_{i-1} + 3f_i\right)^2 / 4. \end{cases} \tag{8}$$

with the ideal weights $d_0 = 3/10,\ d_1 = 3/5,\ d_2 = 1/10.$

The WENOM scheme (Henrick et al. [8]) introduces, $\tilde{\omega}_r^M$, mappings of the weights, that converge faster to their optimal values $d_r$:

$$\tilde{\omega}_r^M = \tilde{\omega}_r \ / \sum_{i=0}^{2} \tilde{\omega}_i\ ,\ \tilde{\omega}_r = g_r(\omega_r),\ r = \overline{0, 2}, \tag{9}$$

where:

$$g_r(\omega) = \frac{\omega(d_r + d_r^2 + 3d_r\omega + \omega^2)}{d_r^2 + \omega(1 - 2d_r)}. \tag{10}$$

The WENOM scheme recovers the optimal order of convergence for smooth problems with critical points but the primary drawback of the mapping is the additional computational cost of the mapping function. High order WENO schemes using non-compact interpolation require large stencils that may lead to loss of accuracy and oscillatory solutions. In addition, they suffer from poor spectral properties.

Therefore, in Compact Reconstruction Weighted Essentially Non-Oscillatory (CRWENO), proposed by Ghosh and Baeder [9], the candidate stencils are compact with implicit interpolation. There are $k$ candidate compact stencils at an interface for a $k$ -th order interpolation.

Optimal weights exist for each stencil such that their combination yields a $(2k$ -1)-th order compact interpolation.

The fifth-order CRWENO scheme is constructed by identifying three third-order compact interpolation schemes at a given interface:

$$\begin{cases} 2\hat{f}_{j-1/2}/3+\hat{f}_{j+1/2}/3=(f_{j-1}+5f_j)/6, \\ \hat{f}_{j-1/2}/3+2\hat{f}_{j+1/2}/3=(5f_j+f_{j+1})/6, \\ 2\hat{f}_{j+1/2}/3+\hat{f}_{j+3/2}/3=(f_j+5f_{j+1})/6. \end{cases} \tag{11}$$

Each equation from (11) is multiplied with optimal weights $c_1$, $c_2$ and $c_3$, respectively. The weighted sum of these interpolation schemes becomes:

$$\begin{aligned} &\frac{c_1}{3}(2\hat{f}_{j-1/2}+\hat{f}_{j+1/2})+\frac{c_2}{3}(\hat{f}_{j-1/2}+2\hat{f}_{j+1/2})+ \\ &+\frac{c_3}{3}(2\hat{f}_{j+1/2}+\hat{f}_{j+3/2})=\frac{c_1}{6}(f_{j-1}+5f_j)+\frac{c_2}{6}(5f_j+f_{j+1})+\frac{c_3}{6}(f_j+5f_{j+1}). \end{aligned} \tag{12}$$

and must be equal with results in a fifth-order accurate compact interpolation scheme:

$$\frac{3}{10}\hat{f}_{j-1/2}+\frac{6}{10}\hat{f}_{j+1/2}+\frac{1}{10}\hat{f}_{j+3/2}==\frac{1}{30}f_{j-1}+\frac{19}{30}f_j+\frac{10}{30}f_{j+1}. \tag{13}$$

The new optimal weights result as $c_1=0.2,\ c_2=0.5, c_3=0.3.$ The CRWENO5 scheme is obtained by replacing the optimal weights $c_k$ in (12) with nonlinear WENO weights $\omega_k$ (n.b. optimal WENO weight $d_k$ is replaced by the new optimal CRWENO weight $c_k$ ). It is obtained a tri-diagonal system:

$$\begin{aligned} &(\frac{2}{3}\omega_1+\frac{1}{3}\omega_2)\hat{f}_{j-1/2}+[\frac{1}{3}\omega_1+\frac{2}{3}(\omega_2+\omega_3)]\hat{f}_{j+1/2}+ \\ &+\frac{1}{3}\omega_3\hat{f}_{j+3/2}=\frac{\omega_1}{6}f_{j-1}+\frac{5(\omega_1+\omega_2)+\omega_3}{6}f_j+\frac{\omega_2+5\omega_3}{6}f_{j+1} \end{aligned} \tag{14}$$

The numerical flux $\hat{f}_{j+1/2}$ is obtained by the WENO-type reconstruction schemes. For stability, it is important that up-winding is used in constructing the flux. An easy and an inexpensive way to achieve up-winding is the Lax-Friedrichs splitting method, in which $f^{\pm}(u)=0.5[f(u)\pm\alpha u]$ and $\alpha=\max_u|f'(u)|$.

## 3. TEMPORAL DISCRETIZATION

As shown before, the numerical solution of the scalar conservation law is semi-discretized in the spatial domain using a discrete set of points and after the spatial partial derivatives have been replaced with appropriate finite differences in $x_j$, we get a system of ODE:

$$\frac{\mathrm{d}\mathbf{u}}{\mathrm{d}t} = L(\mathbf{u}(t)),\ L(u_j) = -\frac{f\left(u(x_{j+1/2},t)\right) - f\left(u(x_{j-1/2},t)\right)}{\Delta x}, \tag{15}$$

where the discrete operator $L$ is used to solve each ODE in time. Here, we associate the time dependent vector $\mathbf{u}(t)$ with $u_j(t) = u(x_j,t),\ j = \overline{0,N}$.

In order to improve the dissipation and dispersion errors for different wave number, the time marching scheme employed in the present paper is the 4-6 Low Dispersion and Dissipation Runge-Kutta (LDDRK) proposed by Hu et al.[12]. The 4-6 notation signifies a two-step marching cycle. Thus, a Standard Runge-Kutta with four stages classical (SRK4) is used for the odd time step and a six stage LDDRK6 for the even time step in the cycle.

An explicit low storage p-stage Runge-Kutta can be expressed as follows:

$$\begin{aligned} \mathbf{u}^{(0)} &= \mathbf{u}^n, \\ \mathbf{u}^{(s)} &= \mathbf{u}^n + c_s \Delta t L(\mathbf{u}^{(s-1)}),\ s = 1,\ldots,p, \\ \mathbf{u}^{n+1} &= \mathbf{u}^{(p)} \end{aligned} \tag{16}$$

where $\mathbf{u}^n$ represent the solution at time $t_n$. The first four coefficients $c_s$ for SRK4 and LDDRK6 are $c_1 = 1, c_2 = 1/2, c_3 = 1/3, c_4 = 1/4$, and last two coefficients for LDDRK6 are $c_5 = 0.1874412,\ c_5 = 0.169193539.$

According to Hu [12], the scheme is a fourth-order accurate scheme in time for a linear problem and second-order accurate for a nonlinear problem. Alternating these schemes, the dispersion and the dissipation errors can be reduced and higher order of accuracy can be maintained.

## 4. NUMERICAL TESTS

In this section we test and compare three selected WENO-type schemes of fifth order (WENO5, WENOM5 and CRWENO5), for nonlinear flux function. Let us consider eq. (1) with Riemann initial condition.

### 4.1 Convex flux

First, we consider the inviscid Burgers equation, $f(u) = u^2/2$, with a piecewise constant initial conditions $u(x,0) = 1 + H(x-1) - 2H(x-2),\quad 0 \le x \le 6.$ We chose this Cauchy condition because the analytical solution has different forms depending on the interval of time. The exact solution is given analytically for three different periods of time:

$$u(x, t \le 1) = \begin{cases} 1, & x - 1 \le t; \\ (x-1)/t, & t < x - 1 < 2t; \\ 2, & 2t \le x - 1 \le 1 + t; \\ 0, & x - 1 > 1 + t, \end{cases} \tag{17}$$

$$u(x,t\le 4)=\begin{cases}1, & x-1<t;\\ (x-1)/t, & t<x-1<2\sqrt{t};\\ 0, & x-1>2\sqrt{t},\end{cases}\quad u(x,t>4)=\begin{cases}1, & x<3+t/2;\\ 0, & x>3+t/2.\end{cases} \tag{18}$$

Therefore it is important to see if the numerical methods predict in an accurate way the solution. For discontinuous initial conditions only the weak solution can be determined [13]. But the weak solution with discontinuities is not unique.

For a convex function $f[u(x,t)]$, the weak solution of eq. (1), is either a shock wave or an expansion wave. To eliminate the physically less realistic solutions by the entropy condition, $f'(u_L)>\sigma>f'(u_R)$ is imposed [14]. Here, $f'(u_L)$ and $f'(u_R)$ represent the speed of the wave to the left and to the right of the discontinuity and $\sigma=(f(u_R)-f(u_L))/(u_R-u_L)$ is the local velocity of the discontinuity.

In this paper the interest is to test the accuracy of methods to predict the interaction between pure or combined waves. Therefore, we consider an example of two adjacent Riemann problems where we can obtain not only a pure wave like in classical Riemann problem, but an interaction of both shock and rarefaction waves after a finite time. Figs 1-4 show the simulation results obtained for different time values: $T=0$, $T=0.5$, $T=2.25$ and $T=4.5$, respectively.

The initial CFL is 0.5 for the grid of 400 points. Predictions given by the WENO-type schemes are indistinguishable at the scale shown. Nevertheless, the numerical solution displays a gradual departure from the analytical solution in the regions with sharp slopes.

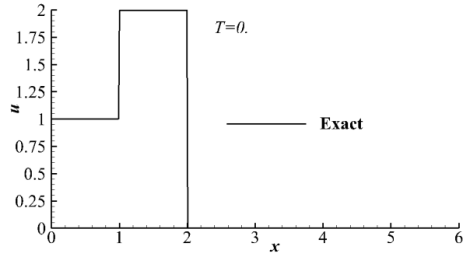


Fig. 1 Solution of Burgers equation at $T$=0

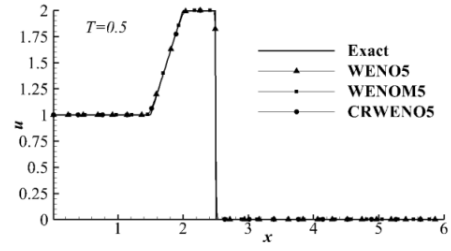


Fig. 2 Solution of Burgers equation at $T$=0.5

At $T=0.5$ the configuration is a succession of three constant values and between them a rarefaction fun and a shock. At $T=2.25$ the configuration is reduced to a combination of two waves, fun and a shock placed between constant areas. Finally at $T=4.5$ the configuration reduces to simple shock wave.

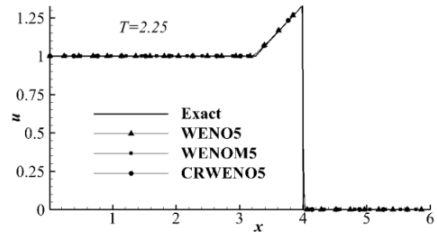


Fig. 3 Solution of Burgers equation at $T$=2.25

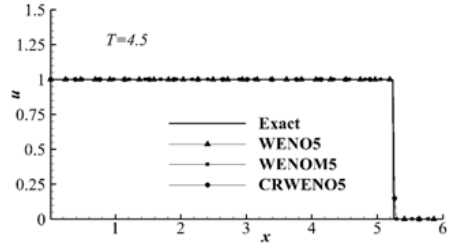


Fig. 4 Solution of Burgers equation at $T$=4.5

### 4.2 Non-convex flux

The weak formulation of a nonlinear conservation law leads to a problem that allows for an infinite number of solutions. In the non-convex flux case, the entropy condition is not enough to guarantee uniqueness of weak solutions. For this reason, a stronger selection criterion is necessary to select the physically relevant discontinuous solution. One of these entropy criteria, which determine the unique entropy weak solution, is Oleinik's jump entropy condition requiring that for all $u$ between $u_r$ and $u_l$:

$$\frac{f(u)-f(u_l)}{u-u_l} \geq \frac{f(u_r)-f(u_l)}{u_r-u_l} \geq \frac{f(u_r)-f(u)}{u_r-u}, \tag{19}$$

where the values $u_r, u_l$ are the local values at the sides of the discontinuity and must not to be interpreted either as the initial values of a Riemann $u_L, u_R$. A shock is an admissible solution if it satisfies the Oleinik entropy condition. From the geometrical point of view, this condition is satisfied if and only if, the chord joining the points $(u_r, f(u_r))$ and $(u_l, f(u_l))$ remains above the graph of $f$ for $u_r < u_l$ and below the graph for $u_r > u_l$. In the non-convex case, distinct from the convex one, it is possible for the solution of the Riemann problem to obtain a wave that is not only a single, individual, shock or fan but a combination of these two types of waves. Between such nonlinear waves we have considered two different non-convex fluxes: one given by Buckley–Leverett [6, 13] with one inflection point (Fig.5) and the other gave by Harten [4, 5] with two inflection points (Fig. 6). The composite waves can be made up by the conjunction of either two or three elementary waves.

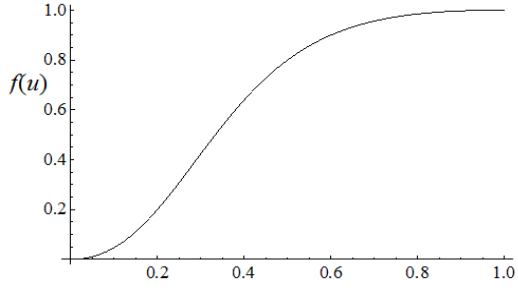


Fig. 5 The Buckley–Leverett flux

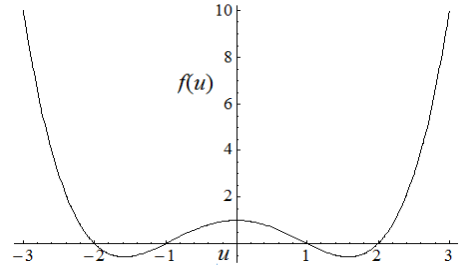


Fig. 6 The Harten flux

**Non-convex flux with one inflection point. The Buckley–Leverett problem.** The classical Buckley-Leverett (BL) equation is an effective model for two-phase (oil-water) fluid flow in a porous medium. One important application area is secondary oil recovery, in which water (with some additives) is pumped down one well in an effort to force more oil out. In this case, $0 \leq u(x,t) \leq 1$ represent the saturation of water ($u=0$ pure oil, $u=1$ pure water). A less complicated non-convex flux is that associated with BL problem where the flux has only one inflection point and is often considered to introduce the idea of convex envelope, which is fundamental in the solution of non-convex Riemann problems, see, for more details [13, 15]. First, we tested all the WENO–type schemes on $x \in [-1,1]$, considering $f(u) = 4u^2 / \left[4u^2 + (1-u)^2\right]$, Fig.5, with the initial condition:

$$u(x,0) = 1 - H(x-1). \tag{20}$$

All the simulations were ruled at $N = 400$ grid points and for CFL=0.5. The solution profile consists in two different double composite waves: fan-shock, see Fig.7.

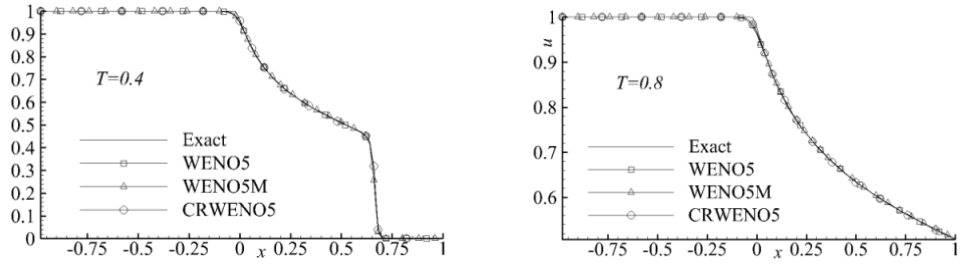


Fig. 7 The Buckley–Leverett solution for initial condition (20) at $T$=0.4 and $T$=0.8

The first wave consists of a fan, from left state $u_L = 1$ to an intermediate state, $u_R^* = 0.447213595499958$ .

This intermediate state is the abscissas of the point of tangency to the flux curve, from $u_R = 0$ obtain by solving numerical:

$$f'(u_R^*) = [f(u_R^*) - f(u_R)] / (u_R^* - u_R) . \tag{21}$$

The fan wave is followed by a shock wave moving with the speed $f'(u_R^*) = 1.61803398874989$ .

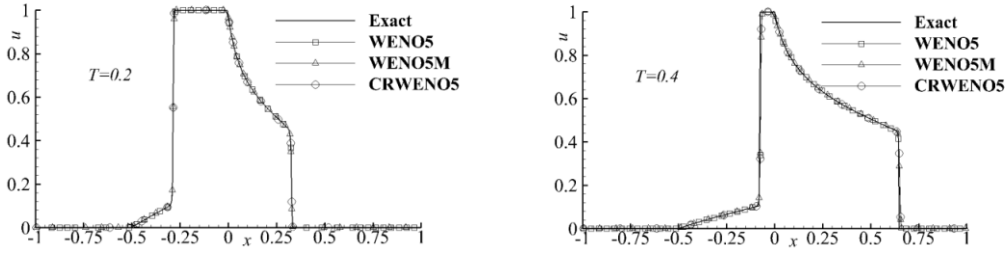


Fig. 8 The Buckley–Leverett solution for second test at $T$=0.2 and $T$=0.4

The analytical wave configuration at any time is represented by the expression

$$u(x,t) = \begin{cases} u_L, & x/t < f'(u_L); \\ G(x/t), & f'(u_L) < x/t < f'(u_R^*); \\ u_R, & x/t > f'(u_R^*). \end{cases} \tag{22}$$

The second test corresponding to the initial condition $u(x,0) = H(x+0.5) - H(x)$ is a succession of two rarefaction-shock waves, see Fig.8.

A fan going from the left state $u_1$ to an intermediate state $u_1^*$ (abscissas of the point of tangency to the flux curve, from $u_1$) and a shock from $u_1^*$ to the central state $u_2$ moving with the velocity $\frac{1}{2}\left( f'(u_1) + \frac{f(u_1^*) - f(u_2)}{u_1^* - u_2} \right) = 1.05901699437495$ where $u_1 = 0$ and $u_2 = 1$ .

The results are compared with the analytically solution which has the expression:

$$u(x,t)=\begin{cases} u_1, & \dfrac{x+0.5}{t} < f'(u_1); \\ G\left(\dfrac{x+0.5}{t}\right), & f'(u_1) \le \dfrac{x+0.5}{t} < \dfrac{f'(u_1)+n}{2}; \\ u_2, & \dfrac{f'(u_1)+n}{2} \le \dfrac{x}{t} \le f'(u_2); \\ G\left(\dfrac{x}{t}\right), & f'(u_2) < \dfrac{x}{t} < f'(u_1^*); \\ u_1, & \dfrac{x}{t} \ge f'(u_1^*). \end{cases} \tag{23}$$

The intermediate state $u_1^*$ is computed by solving the equation $f'(u_1^*)=[f(u_1^*)-f(u_1)]/(u_1^*-u_1)$ numerically.

Analyzing the results presented in Figs. 7-8, we can conclude that WENO-type schemes converge to the correct analytically entropy solution and they give sharp shock profile. Note that, around discontinuities, all schemes predict approximately the same evolution.

**Non-convex flux with two inflection point. The Harten problem.** The problem proposed by Harten [6] is defined by a fourth-order polynomial, $f(u)=0.25(u^2-1)(u^2-4)$, Fig.6, and has two inflection points because of the expression: $f''(u)=3u^2-2.5$. The numerical tests are performed for two different initial Riemann conditions $u_L=2, u_R=-2$ and $u_L=-3, u_R=3$, respectively.

The exact solution in this case is

$$u(x,t)=\begin{cases} u_L, & x/t < f'(u_L^*); \\ G(x/t), & f'(u_L^*) < x/t < f'(u_R^*); \\ u_R, & x/t > f'(u_R^*), \end{cases} \tag{24}$$

where the intermediate state $u_L^*$, $u_R^*$ are obtained solving numerically: $f'(u_R^*)=[f(u_R^*)-f(u_R)]/(u_R^*-u_R)$, $f'(u_L^*)=[f(u_L^*)-f(u_L)]/(u_L^*-u_L)$ and the self-similar weak solution satisfies $G=(f')^{-1}$.

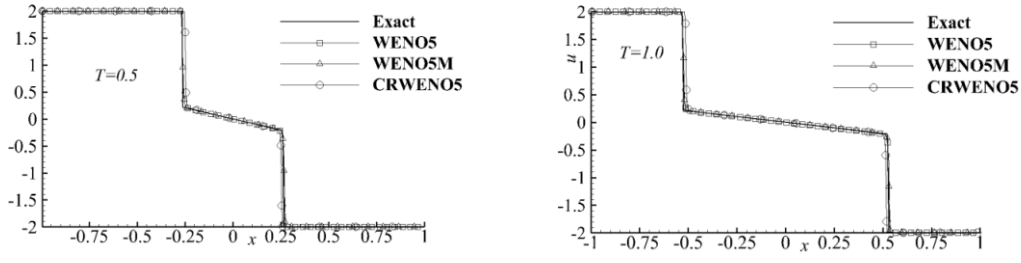


Fig. 9 Solution of Harten problem, $u_L=2, u_R=-2$ at $T=0.5$ and $T=1.0$

The occurrence of two inflection points implies that the solution in both cases is a mixture comprising three pure waves in the two different configurations. The first pattern for a triple wave, given by the first initial condition is obtained by the combination of a shock followed by a fan and a second shock, see Figs 9-10 at $T = 0.5$ and $T = 1.0$.

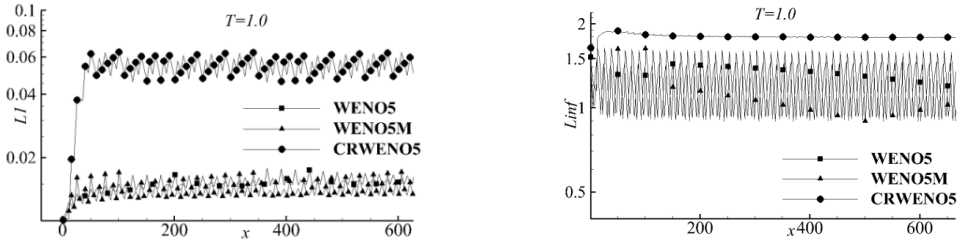


Fig. 10 Errors $L_1$ and $L_\infty$ for Harten problem solutions, $u_L = 2, u_R = -2$ at $T = 1.0$

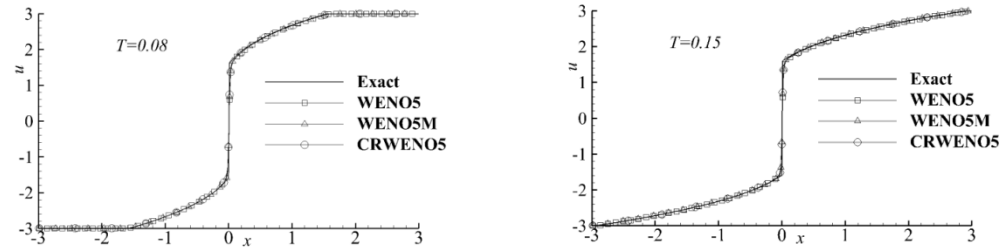


Fig. 11 The Harten problem solution for $u_L = -3, u_R = 3$ at $T = 0.08$ and $T = 0.15$

The last initial condition produces a wave configuration; referred to two external rarefactions with a single jump located in between, see Figs 11-13. We carried out the computation up to $T = 0.15$.

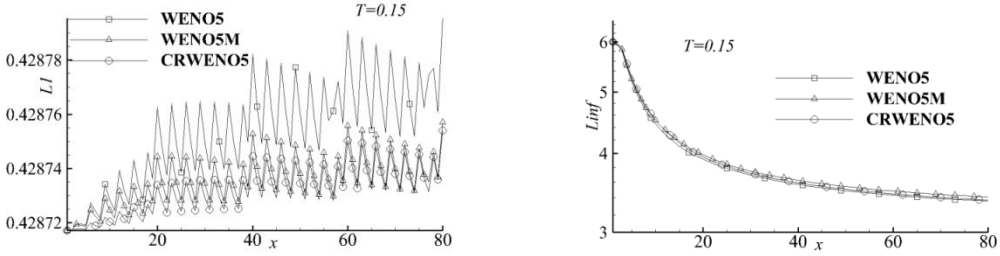


Fig. 12 The $L_1$ and $L_\infty$ error Harten problem solution for $u_L = -3, u_R = 3$ at $T = 0.15$

The exact solution in this case is

$$u(x,t) = \begin{cases} u_L, & x/t < f'(u_L); \\ G_1(x/t), & f'(u_L) < x/t < f'(u_L^e); \\ G_2(x/t), & f'(u_R^e) < x/t < f'(u_R); \\ u_R, & x/t > f'(u_R), \end{cases} \tag{25}$$

where $u_L^e$, $u_R^e$ are the points in which a single straight line is tangent to the flux curve in two points simultaneously to obtain a convex envelope for the flux curve[12]. Functions $G_1$, $G_2$ verify the condition $G = (f')^{-1}$.

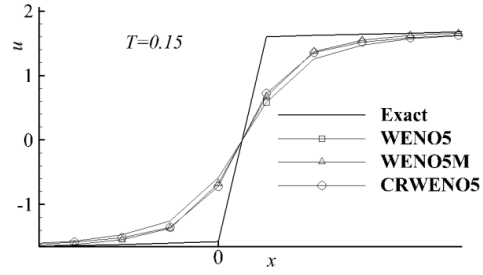


Fig. 13 The detailed Harten problem solution for $u_L = -3, u_R = 3$ at $T = 0.15$

## 5. CONCLUSIONS

The most known fifth order WENO-type schemes presented in the previous section are simultaneously analyzed for the first time. Their behavior, in terms of accuracy and convergence properties, was studied for one convex and two non-convex conservative fluxes. Thus, the Buckley-Leverett and the Harten problems are two examples of non-convex flux with one and respectively two inflection points. The schemes were tested on piecewise constant function for non-periodical conditions. The exact solution for each problem is provided in analytical form. Sometimes, the specialized literature is biased towards cases that are favorable to a certain method. Our approach tried to objectively present the performance of each method for simple cases like scalar conservation law problems. All the schemes identify accurately the position of the shock and converge to the proper weak solution for non-linear flux and different initial conditions. However, for real fluid simulations, we would suggest the use of WENOM5 scheme as a good compromise between WENO5 and CRWENO5, even if CRWENO scheme gives more accurate results but at higher CPU costs.

## REFERENCES

[1] A. Bogoi, D. Isvoranu, S. Dănăilă, Assessment of some high-order finite difference schemes on the scalar conservation law with periodical conditions, *INCAS BULLETIN*, vol. **8**, issue 4, (online) ISSN 2247–4528, (print) ISSN 2066–8201, ISSN–L 2066–8201, DOI: 10.13111/2066-8201.2016.8.4.7, pp.77 – 92, 2016.

[2] S. Dănăilă, A. Bogoi, D. Isvoranu, Some Mandatory Benchmark Tests for Stability and Accuracy of High-Order Finite Difference Schemes, *Applied Mechanics and Materials*, vol. **859**, pp. 52-56, 2017.

[3] R. J. Leveque, *Finite Volume Methods for Hyperbolic Problems*, Cambridge University Press, 2002.

[4] D. Ballou, Solutions to Nonlinear Hyperbolic Cauchy Problems without Convexity Conditions, *Transactions of the American Mathematical Society*, vol. **152**, pp. 441-460, 1970.

[5] O. A. Oleinik, On the Cauchy problem for weakly hyperbolic equations, *Comm. pure appl. math*., vol. 23, pp. 569–586, 1970.

[6] A. Harten, B. Engquist, S. Osher, S. R. Chakravarthy, Uniformly high order accurate essentially non-oscillatory schemes, III, *Journal of Computational Physics*, vol. **71**, pp. 231–303, 1987.

[7] C.-W. Shu, S. Osher, Efficient implementation of essentially non-oscillatory shock capturing schemes II, *Journal of Computational Physics*, vol. **77**, pp. 439, 1988.

[8] A. K. Henrick, T. D. Aslam, J. M. Powers, Mapped weighted essentially non-oscillatory schemes: achieving optimal order near critical points, *Journal of Computational Physics*, vol. **207**, pp. 542–567, 2005.

[9] D. Ghosh, J. D. Baeder, Compact Reconstruction Schemes with Weighted ENO Limiting for Hyperbolic Conservation Laws, *SIAM Journal on Scientific Computing*, vol. **34**, pp. 1678–1706, 2012.

[10] G.-S. Jiang, C.-W. Shu, Efficient implementation of weighted ENO schemes, *Journal of Computational Physics*, vol. **126**, pp. 202–228, 1996.

[11] C. Bogey, C. Bailly, A Family of Low Dispersive and Low Dissipative Explicit Schemes for Computing the Aerodynamic Noise, *AIAA-paper 2002-2509*, 2002.
[12] F. Q. Hu, M. Y. Hussaini, J. L. Manthey, Low-dissipation and low-dispersion Runge-Kutta schemes for computational acoustics, *Journal of Computational Physics*, vol. **124**, pp. 177-191, 1996.
[13] S. Dănăilă, C. Berbente, *Metode numerice în dinamica fluidelor (Numerical Methods in Fluid Dynamics)*, Ed. Academiei, 2003.
[14] E. Godlewski, P.-A. Raviart, *Numerical Approximation of Hyperbolic Systems of Conservation Laws*, Springer Verlag, New York, 1996.